COMMUNICATION

Deciphering iron-dependent activity in oxygen evolution catalyzed by nickel iron layered double hydroxide

Seunghwa Lee, Lichen Bai, Xile Hu*[a]

[a] Dr. S. Lee, L. Bai, Prof. Dr. X. L. Hu
Laboratory of Inorganic Synthesis and Catalysis
Institute of Chemical Sciences and Engineering, Ecole Polytechnique Fédérale de Lausanne (EPFL)
1015 Lausanne (Switzerland)
E-mail: xile.hu@epfl.ch
Homepage: http://lsci.epfl.ch

Supporting information for this article is given via a link at the end of the document.

Abstract: Nickel iron oxyhydroxide is the benchmark catalyst for the oxygen evolution reaction (OER) in alkaline medium. Whereas the presence of Fe ions is essential to the high activity, the functions of Fe are currently under debate. Using oxygen isotope labelling and operando Raman spectroscopic experiments, we obtain turnover frequencies (TOFs) of both Ni and Fe sites for a series of Ni and NiFe layered double hydroxides (LDHs), which are structurally defined samples of the corresponding oxyhydroxides. The Fe sites have TOFs 20-200 times higher than the Ni sites such that at an Fe content of 4.7% and above the Fe sites dominate the catalysis. Higher Fe contents lead to larger structural disorder of the NiOOH host. A Volcano-type correlation was found between the TOFs of Fe sites and the structural disorder of NiOOH. Our work elucidates the origin of the Fe-dependent activity of NiFe LDH, and suggests structural ordering as a strategy to improve OER catalysts.

The oxygen evolution reaction (OER) is the oxidative half reaction of water splitting. OER is considered as the bottle neck of water splitting.[1] Efficient and scalable OER catalysts are required to make water splitting a viable solution for energy storage.[1a, 1b, 2] A tremendous amount of efforts have been made to develop OER catalysts. Nickel iron oxyhydroxide ($NiFeO_x$) is now recognized as a benchmark catalyst for OER in alkaline medium.[1b, 3] Whereas the high catalytic activity of $NiFeO_x$ is well established, questions related to the origin of its activity as well as the nature of the active site remain unresolved. In particular, there is a vivid debate on whether Ni or Fe sites serve as the active sites.[4] Previous experimental studies focused on spectroscopic evidences for Ni- or Fe-based active sites.[4a, 4d, 4e, 4i-k, 4n, 5] These evidences tend to be indirect, and their interpretations are equivocal. Here we report the determination of the intrinsic activity of both Ni and Fe sites in NiFe layered double hydroxide (LDH), which is a structurally defined form of $NiFeO_x$. Analysis of the site-specific activity in Ni and NiFe LDH samples with different Fe contents reveals the origin of the Fe-dependent activity of NiFe LDH.

We are able to deconvolute the total OER activity of NiFe LDH into that of Ni and Fe sites thanks to their different behaviors in oxygen isotope exchange experiments. Using operando Raman spectroscopy, we previously found that Ni sites evolve O_2 through an active oxygen species (Ni-O-O·) and with lattice oxygen participation, whereas Fe sites evolve O_2 without lattice oxygen participation and not through an active oxygen species.[4a] When OER occurs through Ni sites, the lattice O will exchange with the O atoms of the OH^- electrolyte. On the other hand, when OER occurs through Fe sites, there is no exchange of lattice O with OH^-. The degree of O exchange can therefore be correlated to the percentage of Ni-based activity.

We prepared Ni and NiFe LDH nanosheets with different compositions by a modified literature method.[4a, 6] The compositions were determined by inductively coupled plasma-optical emission spectrometry (ICP-OES, Table S1). We chose seven samples with Fe contents from 0% to 28% to cover a wide range of composition space. Transmission electron microscopy (TEM) images (Figure S1) show that all LDH samples consist of ultrathin nanosheets with a lateral size of 10-50 nm. The observed Tyndall effect (Figure S2) of colloidal suspensions of the LDH nanosheets indicates a good dispersion of the nanosheets.[4a, 7]

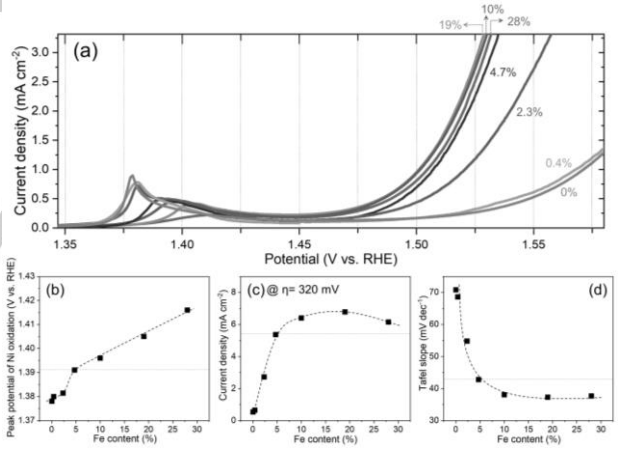

Figure 1. (a) Linear sweep voltammograms of NiFe LDH samples with various Fe contents recorded at a scan rate of 1 mV s^{-1} in Fe-free 0.1 M KOH. Comparison of (b) anodic peak potentials of Ni^{2+} to Ni^{3+}, (c) current densities at overpotential of 320 mV, and (d) Tafel slope.

The apparent geometric OER activity of the LDH samples was measured by linear sweep voltammetry at a scan rate of 1 mV s^{-1} in Fe-free 0.1 M KOH solutions. The LSV curves exhibit significantly different features depending on the amount of Fe ions (Figure 1a). Two pronounced oxidation features were observed. Oxidation peaks at lower potentials (1.35 to 1.45 V vs. RHE) correspond to the transformation of $Ni(OH)_2$ to NiOOH, while oxidations at higher than 1.45 V are due to OER.[1a, 1b, 7-8] The peak potential of the $Ni(OH)_2$ to NiOOH transformation, typically assigned as Ni(II) to Ni(III), shifted to high values with increasing Fe content (Figure 1b). This result is consistent with previous

studies suggesting the suppression of Ni(II) to Ni(III) oxidation by Fe dopants.[8b, 9] The suppression becomes consequential at an Fe content of 4.7%. The geometric activity, as exemplified by current densities at an overpotential (Π) of 320 mV (Figure 1c), first increased significantly from 0% Fe to 4.7% Fe. Further increase of Fe content led to smaller and non-linear change in the activity. The Tafel slopes followed a similar trend (Figure 1d). The slope was about 71 mV dec^{-1} in samples containing 0 or 0.4% Fe, and dropped rapidly to about 43 mV dec^{-1} at an Fe content of 4.7%. The slope decreased slightly to a saturated value of about 38 mV dec^{-1} with higher Fe contents. An Fe content of about 19% gave an optimal geometric activity. The dependence of geometric activity on Fe content found here is largely in agreement with previous studies on various samples and forms of NiFe oxyhydroxides.[4c, 4d, 5b, 5c].

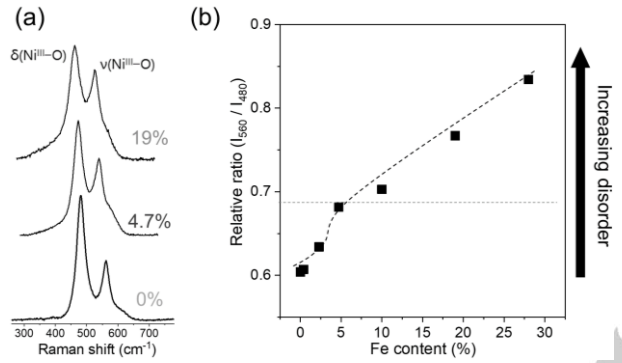

Figure 2. (a) In-situ Raman spectra of NiFe LDHs containing Fe 0%, 4.7% and 19% collected at 1.65 V (vs. RHE) in 0.1 M Fe-free KOH. (b) Intensity ratio of peaks corresponding to bending (480 cm^{-1}) and stretching (560 cm^{-1}) vibrations of Ni-O in NiOOH denoted as I_{560}/I_{480}.

Operando Raman spectra of these samples were collected in the potential range from open circuit potential (ocp) to 1.65 V with an interval of 0.05 V (Figures 2a and S3-4). Upon the first oxidation of $Ni(OH)_2$ to NiOOH, a pair of bands emerged at around 480 and 560 cm^{-1}. The peaks at 560 cm^{-1} and 480 cm^{-1} have been assigned to the polarized A_{1g} mode (strechting) and the depolarized E_g mode (bending) of γ-NiOOH, respectively.[4c, 5c, 10] For the A_{1g} mode the oxygen atoms vibrate perpendicular to the oxygen plane whereas for the E_g mode the oxygens vibrate along this plane (Figure S4h).[10b, 10c] The intensities and positions of these peaks reflect the changes in local structure of Ni-O such as lattice disorder within sheets and interlayer spacing between the sheets.[5c, 10c] The broad feature in frequencies from 800-1200 cm^{-1} (Figure S4) also appeared. The high frequency feature was previously assigned to a superoxidic species, also called active oxygen (OO^-).[4a, 4c, 4k, 5c, 11] The intensity ratio of the two Ni-O peaks, denoted as I_{560}/I_{480}, increased with increasing Fe content (Figure 2b). The I_{560}/I_{480} ratio was previously correlated to structural disorder of NiOOH, and a higher ratio indicated higher structural disorder.[4c, 5b, 5c] Additionally, Ni-O stretching band (at 560 cm^{-1} in Fe-free sample) shifted to lower frequencies with increasing Fe content (Figure S3b). This shift was previously correlated to an elongation of the Ni-O bonds.[4c, 10c] Thus, the Raman data indicate higher structural disorder of NiOOH and longer Ni-O bonds with increasing Fe content. Previous work suggested the formation of a γ-FeOOH phase in electrodeposited $NiFeO_x$ at high Fe contents (>25%).[4d] We did not observe features associated with γ-FeOOH in our Raman measurements for LDH samples with Fe contents of up to 28%.

The above electrochemical and Raman data indicate that the LDH samples with an Fe content of 4.7% and higher are similar among themselves, but distinct from those with a lower Fe content. The samples with Fe contents from 0.4 to 4.7% are a good representation of the various forms of NiFe LDHs.

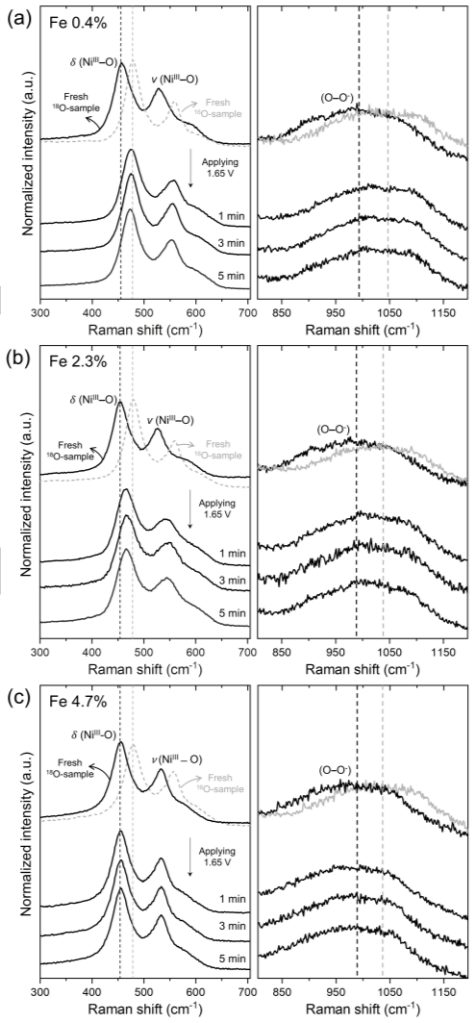

Figure 3. Oxygen isotope exchange experiments. In-situ Raman spectra of ^{18}O-labelled NiFe LDHs containing (a) Fe 0.4%, (b) 2.3% and (c) 4.7% acquired at 1.65 V in Fe-free 0.1 M $H_2{}^{16}O$ solution of $K^{16}OH$. The Raman spectra are shown in the frequency regions of NiOOH (left column) and OO^- (right column). Peaks from ^{16}O-labelled samples are colored coded.

We subjected three NiFe LDHs, with an Fe content of 0.4, 2.3, and 4.7%, respectively, to oxygen isotope labelling experiments.[4a] The lattice oxygens of freshly prepared LDHs were first labelled with ^{18}O by applying an electrical potential of 1.65 V for 3 min in 0.1 M Fe-free $H_2{}^{18}O$ solution of $K^{18}OH$. After this treatment, the two main peaks of NiOOH at 480 and 560 cm^{-1} shifted to lower frequencies by ~23 cm^{-1} (Figure 3, left) and the broad spectrum associated with $NiOO^-$ in 800-1200 cm^{-1} was red-shifted by ~50 cm^{-1} (Figure 3, right), confirming the isotope exchange.[4a, 11] The Fe-free $H_2{}^{18}O$ solution of $K^{18}OH$ was then

replaced by a Fe-free $H_2{}^{16}O$ solution of $K^{16}OH$. Electrolysis was conducted at 1.65 V for 5 min. We previously reported that for Ni LDH, both lattice O and O-O$^-$ in the ^{18}O-labelled was exchanged back to ^{16}O in the electrolysis, indicating the involvement of lattice O and O-O$^-$ in OER.[4a] For NiFe LDH with 25% Fe, neither lattice O and O-O$^-$ in the ^{18}O-labelled was exchanged back to ^{16}O in the electrolysis, indicating a different active site, likely at the surface and based on Fe.[4a] In the current study, for NiFe LDH containing 0.4% Fe, the Raman peaks corresponding to NiOOH and OO$^-$ shifted back near to the positions for a fresh ^{16}O-labelled sample (Figure 3a). The shifts were nearly identical to those of pure Ni LDH.[4a] For NiFe LDH with 2.3% Fe, the peaks of Ni-O and OO$^-$ shifted to positions half-way between those of ^{16}O- and ^{18}O-labelled samples (Figure 3b). For NiFe LDH with 4.7% Fe, the peaks of Ni-O and OO$^-$ remained at the original positions of ^{18}O-labelled sample (Figure 3c). The data in Figure 3 indicate that for NiFe LDH, the Ni site remained relevant for an Fe content of up to 2.3%. At an Fe content of 4.7% and above, a second site previously proposed as a surface Fe site,[4a, 4c, 4d, 4f, 4g, 9] becomes the dominant active site.

Table 1. Comparison of TOFs of Ni, NiFe and NiCr LDHs at η = 320 mV.

	TOF (s^{-1})		
Sample	**Ni-site**	**Fe-site**	**total metal site**
Fe 0%	0.018	-	0.018
Fe 0.4%	0.022	-	0.022
Fe 2.3%	0.061	1.3	0.098
Fe 4.7%	-	3.8	0.179
Fe 10%	-	2.1	0.210
Fe 19%	-	1.2	0.228
Fe 28%	-	0.72	0.202
Cr 18%	0.044	-	0.036

Table 1 shows the turnover frequencies (TOFs) at η = 320 mV in different samples. Due to the ultrathin nature of our LDH samples, we assumed all Ni and Fe sites as possible active sites. For Ni and NiFe (0.4% Fe) LDHs, the observed activity was attributed to Ni sites; for NiFe LDH (2.3%), the activity was attributed to both Ni and Fe sites according to the percentage of isotopic shift observed in Figure 3; for NiFe LDHs with an Fe content of 4.7% and above, we attributed all activity to Fe sites (see SI for details). Interestingly, the TOFs of Ni sites increases with Fe doping. Without Fe, the Ni site has a TOF of 0.018 s^{-1}. With 2.3% Fe, the TOF increases to 0.061 s^{-1}. Whether the TOFs of Ni sites further increase with increasing Fe content could not be probed because at a higher Fe content, the Fe sites completely dominate the catalysis. At 2.3% Fe, the Fe sites have a TOF of 1.3 s^{-1}, 22 times higher than the corresponding Ni sites. The highest TOF (3.8 s^{-1}) was obtained at an Fe content of 4.7%. Further increasing the Fe content leads to a gradual decrease of TOFs. The lowest TOF (0.72 s^{-1}) was obtained for an Fe content of 28%. It was proposed that the TOFs at low Fe contents were limited by non-optimal distribution of Fe ions,[4c, 4g] whereas the TOFs at high Fe contents were deteriorated by the formation of inactive γ-FeOOH.[4c, 4d, 4g] The absence of γ-FeOOH in our LDH samples, even at an Fe content of 28%, indicates a different origin for the activity decrease at high Fe contents. For comparison with literature data, we also list TOFs based on total metal sites. In most cases, these TOFs, just like the total currents, do not reflect the intrinsic activity of real active sites.

For a series of $Fe_{100-y}Ni_yO_x$ photochemically deposited on FTO, Fe-induced structural disorder of the active Ni sites was proposed as the main origin of the much higher activity of iron nickel oxyhydroxide compared to nickel oxyhydroxide.[4n] To differentiate the influences of Fe incorporation and structural disorder in OER activity, we studied NiCr LDH, where the Cr ions mimic the Fe ions in NiFe LDH.[12] A NiCr LDH (18% Cr) was synthesized (Figure S5) and characterized (Figures S5 and 6). Similar to Fe, Cr dopant induces structural disorder in the NiOOH host. The NiCr LDH behaves similarly to Ni LDH, but differently from NiFe LDH, in O isotope exchange experiments (Figure S6c), suggesting bulk Ni sites as active sites. The activity of NiCr (TOF: 0.044 s^{-1}, Table 1) is about twice of that of Ni LDH (TOF: 0.018 s^{-1}), but much lower than that of NiFe LDH (TOF: 3.82 s^{-1} for Fe 4.7%). Thus, structural disorder induced by a dopant cannot account for the drastic increase of activity due to Fe incorporation. This result further supports the formation of an Fe-based active site as the origin of the high activity of NiFe LDH.

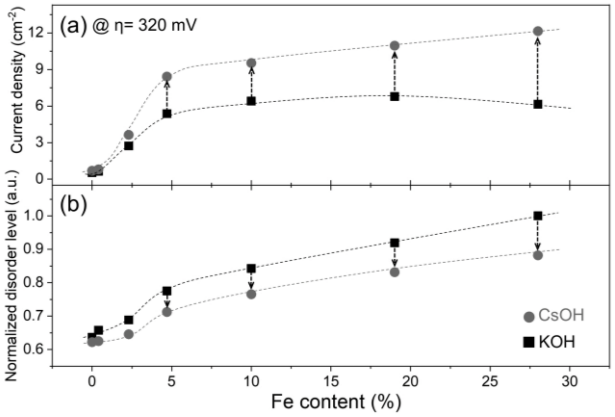

Figure 4. Dependence of (a) current densities measured at overpotential of 320 mV in 0.1 M KOH and CsOH and (b) normalized disorder level based on the relative ratio of two Raman peaks (480 and 560 cm^{-1}) of NiOOH on Fe content.

The structural disorder might play a role in regulating the activity of Fe sites in NiFe LDHs. To probe this, we compared the activity in KOH and CsOH. It was reported earlier that the positions of Raman peaks corresponding to Ni-O bonds of NiOOH red-shifted in CsOH compared to in KOH, which was attributed to structural changes as a result of Cs^+ intercalation.[13] We found that the OER activity increased modestly when changing the electrolyte from KOH to CsOH for samples with Fe contents of 0-2.3% (Figure 4a and Figure S7). However, for NiFe LDHs with an Fe content of 4.7% and above, the Cs^+ cation promoted significantly the catalytic activity. Table S2 shows that the Tafel slopes for the Ni and NiFe LDHs remained similar in KOH and CsOH, indicating similar nature of active sites as well as mechanisms in KOH and CsOH. As the OER activity is mostly due to Ni sites for samples with an Fe content of 2.3% or lower, and due to Fe sites for

samples with a higher Fe content, these data indicate that Cs^+-promotion is more significant for Fe sites. Consistent with this assessment, the activity of NiCr LDH is only modestly increased when replacing KOH with CsOH (Figure S8). In the Raman spectra of all samples, the peaks corresponding to Ni-O bending and stretching modes were shifted to lower frequencies when the electrolyte was shifted from KOH to CsOH (Figures S9-11). This shift indicates an elongation of Ni-O bonds.[13] Notably, the normalized disorder level, based on the peak intensity ratio I_{560}/I_{480},[4c, 5b, 5c] decreased substantially for NiFe LDHs with an Fe content of 4.7% and above (Figure 4b and Figure S10). In view of the synchronous changes in disorder and catalytic activity upon replacement of KOH with CsOH, we attribute a Cs^+-induced ordering of the lattice as the main origin of the significantly higher OER activity of the Fe sites in CsOH compared to in KOH. Other factors previously proposed to explain the cation effect of OER, including enhanced water diffusion in the interlayer space[14] and cation-induced exfoliation[15] can be ruled out because our LDH samples are ultrathin and have abundant accessible surface sites, and because our samples are not exfoliated in CsOH. We can also exclude a stabilizing interaction of $NiOO^-$ with Cs^+ because we did not observe an evolution of a shoulder peak between 930-950 cm^{-1} in CsOH (Figures S12 and 13).[13b] To probe the possibility of electric field effect[16] due to Cs^+ adsorption, we measured OER in tetramethylammonium hydroxide (TMAOH) solution. TMA^+ is larger than Cs^+ and should induce a larger electric field effect. However, TMA^+ did not enhance OER (Figure S14), suggesting that Cs^+-promotion is not due to an electric field effect. In addition, the activity trends recorded in KOH and CsOH remained the same when the solutions were purged with nitrogen to remove oxygen (Figure S15), excluding different oxygen solubility in KOH and CsOH as a factor influencing OER activity.[17]

We correlated the TOFs of Fe sites, the Fe contents, and the normalized disorder level of our samples (Figure 5). As observed above (Figure 2b), a higher Fe content leads to a higher disorder. For each sample, increasing disorder decreases TOF. Thus, the gradual decrease of TOFs with increasing Fe contents for samples with an Fe content of 4.7% and above might be attributed to increasing structural disorder of the NiOOH lattice. The sample with an Fe content of 2.3% is noteworthy. It has the lowest disorder but only modest TOFs compared to other samples. The modest TOFs might be due to trapping of a significant portion of Fe ions in unproductive sites as proposed in previous studies.[4c, 4g] Alternatively, the modest TOFs of this sample indicate a Volcano-type correlation of activity with disorder level for the Fe sites. To probe these possibilities, we conducted experiments on two more samples of NiFe LDHs, with an Fe content of 3.7% and 24%, respectively (Figures S16-18). The TOFs of Fe sites in these two samples fit in the Volcano-type correlation (Figures 5 and S19), supporting the existance of an optimal level of disorder for activity, occuring at around Fe 4.7%. Isotope exchange experiments indicate that at an Fe content of 24%, the activity of Ni sites remain neglibible compared to that of Fe sites (Figure S18).

The geometric activity, with has a relevance to application, is the product of TOF with Fe concentration. Because of the often counter-acting dependence of TOF and disorder in Fe content, the highest geometric activity is obtained in KOH when the Fe content was 19% (Figure S20). Attenuating the disorder using CsOH is more effective for samples with a higher Fe content. The highest geometric activity in CsOH is obtained for the sample with an Fe content of 28%.

Our data indicate more Fe incorporation leads to higher structural disorder of NiOOH, which is consistent with previous reports.[4c, 5b, 5c] However, our analysis suggests structural disorder can be detrimental to the TOFs of Fe sites, while previous work suggested the opposite effect.[4n, 5b, 5c] The discrepancy arise from the different methods employed to calculate the activity. In our study, because we are able to assign activity to either Ni or Fe sites, we obtain the intrinsic activity of relevant active sites (TOFs). Previously geometric activity of the whole samples was used as the parameter of activity, which may not reflect the true activity of active sites.[18]

Our results suggest optimizing lattice order of NiOOH as a strategy to improve the OER activity of NiFe oxyhydroxides. This effect might be achieved using CsOH as the electrolyte as shown here, or by ball milling of samples to induce lattice tensile strain, which also resulted in lattice ordering accordng to Raman spectroscopy.[19] The physical origin of this effect might be an optimization of the adsorption energies of oxygenated intermediates at reactive sites.[20] It is conceivable that for the Fe sites in NiFe LDH, the optimized structures correlate to an optimal disorder level of the NiOOH host, which is on the low end (top of Volcano in Figure 5). The effect of structural ordering might be relevant when comparing the activity of crystalline and amorphous oxide catalysts.[21]

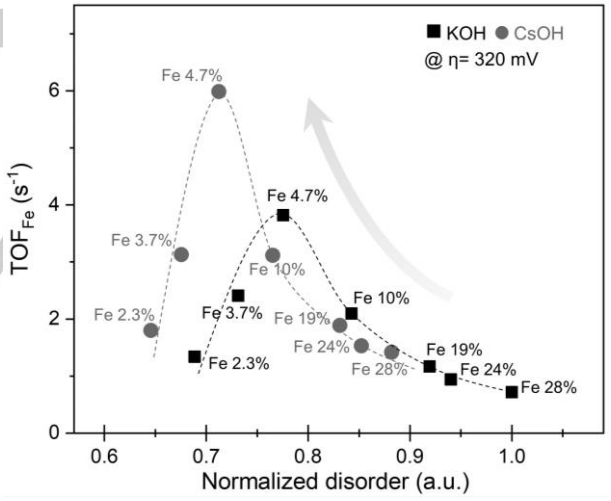

Figure 5. Correlation of TOFs on a per Fe basis acquired at η=320 mV to normalized lattice disorder of NiOOH. The relative intensity of two Raman peaks for Fe 28% in KOH was set to originate from a disorder level of 1.0.

In summary, oxygen isotope labelling and operando Raman spectroscopy allow the determination of TOFs of Ni and Fe sites in OER for a series of Ni and NiFe LDHs with different Fe contents. The TOFs of Fe sites are 20-200 times higher than those of Ni sites. However, due to their higher concentrations, the Ni sites remain catalytically relevant for NiFe LDHs with an Fe content of 2.3%. Incorporation of Fe ions into NiOOH leads to structural disorder, which exhibits a Volcano-type correlation with the activity of Fe sites. Our work clarifies the activity of Ni and Fe sites in LDHs, and suggest structural ordering as a strategy to improve the activity of NiFe oxyhydroxides.

Acknowledgements

This work has received funding from the European Union's Horizon 2020 research and innovation programme under the Marie Skłodowska-Curie Grant Agreement No. 838367 and the ERC Grant Agreement No. 681292.

Keywords: oxygen evolution reaction • nickel iron oxyhydroxide • Raman spectroscopy • electrocatalysis • active site

[1] a) N. T. Suen, S. F. Hung, Q. Quan, N. Zhang, Y. J. Xu, H. M. Chen, *Chem. Soc. Rev.* **2017**, *46*, 337-365; b) F. Song, L. Bai, A. Moysiadou, S. Lee, C. Hu, L. Liardet, X. Hu, *J. Am. Chem. Soc.* **2018**, *140*, 7748-7759; c) H. Dau, C. Limberg, T. Reier, M. Risch, S. Roggan, P. Strasser, *ChemCatChem* **2010**, *2*, 724-761.

[2] a) T. R. Cook, D. K. Dogutan, S. Y. Reece, Y. Surendranath, T. S. Teets, D. G. Nocera, *Chem. Rev.* **2010**, *110*, 6474-6502; b) M. G. Walter, E. L. Warren, J. R. McKone, S. W. Boettcher, Q. Mi, E. A. Santori, N. S. Lewis, *Chem. Rev.* **2010**, *110*, 6446-6473; c) B. M. Hunter, H. B. Gray, A. M. Müller, *Chem. Rev.* **2016**, *116*, 14120-14136.

[3] a) F. Dionigi, P. Strasser, *Adv. Energy Mater.* **2016**, *6*, 1600621; b) M. Gong, H. Dai, *Nano Res.* **2015**, *8*, 23-39; c) C. C. McCrory, S. Jung, J. C. Peters, T. F. Jaramillo, *J. Am. Chem. Soc.* **2013**, *135*, 16977-16987; d) C. Roy, B. Sebok, S. B. Scott, E. M. Fiordaliso, J. E. Sørensen, A. Bodin, D. B. Trimarco, C. D. Damsgaard, P. C. K. Vesborg, O. Hansen, I. E. L. Stephens, J. Kibsgaard, I. Chorkendorff, *Nat. Catal.* **2018**, *1*, 820-829.

[4] a) S. Lee, K. Banjac, M. Lingenfelder, X. Hu, *Angew. Chem. Int. Ed.* **2019**, *58*, 10295-10299; *Angew. Chem.* **2019**, *131*, 10401-10405; b) H. S. Ahn, A. J. Bard, *J. Am. Chem. Soc.* **2015**, *138*, 313-318; c) S. Klaus, Y. Cai, M. W. Louie, L. Trotochaud, A. T. Bell, *J. Phys. Chem. C* **2015**, *119*, 7243-7254; d) D. Friebel, M. W. Louie, M. Bajdich, K. E. Sanwald, Y. Cai, A. M. Wise, M. J. Cheng, D. Sokaras, T. C. Weng, R. Alonso-Mori, R. C. Davis, J. R. Bargar, J. K. Norskov, A. Nilsson, A. T. Bell, *J. Am. Chem. Soc.* **2015**, *137*, 1305-1313; e) J. Y. Chen, L. Dang, H. Liang, .W. Bi, J. B. Gerken, S. Jin, E. E. Alp, S. S. Stahl, *J. Am. Chem. Soc.* **2015**, *137*, 15090-15093; f) J. M. P. Martirez, E. A. Carter, *J. Am. Chem. Soc.* **2018**, *141*, 693-705; g) M. B. Stevens, C. D. Trang, L. J. Enman, J. Deng, S. W. Boettcher, *J. Am. Chem. Soc.* **2017**, *139*, 11361-11364; h) N. Li, D. K. Bediako, R. G. Hadt, D. Hayes, T. J. Kempa, F. Von Cube, D. C. Bell, L. X. Chen, D. G. Nocera, *Proc. Natl. Acad. Sci.* **2017**, *114*, 3050-3055; i) M. Gorlin, J. Ferreira de Araujo, H. Schmies, D. Bernsmeier, S. Dresp, M. Gliech, Z. Jusys, P. Chernev, R. Kraehnert, H. Dau, P. Strasser, *J. Am. Chem. Soc.* **2017**, *139*, 2070-2082; j) M. Gorlin, P. Chernev, J. Ferreira de Araujo, T. Reier, S. Dresp, B. Paul, R. Krahnert, H. Dau, P. Strasser, *J. Am. Chem. Soc.* **2016**, *138*, 5603-5614; k) B. J. Trzesniewski, O. Diaz-Morales, D. A. Vermaas, A. Longo, W. Bras, M. T. Koper, W. A. Smith, *J. Am. Chem. Soc.* **2015**, *137*, 15112-15121; l) Z. K. Goldsmith, A. K. Harshan, J. B. Gerken, M. Vörös, G. Galli, S. S. Stahl, S. Hammes-Schiffer, *Proc. Natl. Acad. Sci.* **2017**, *114*, 3050-3055; m) H. Xiao, H. Shin, W. A. Goddard, *Proc. Natl. Acad. Sci.* **2018**, *115*, 5872-5877; n) R. D. Smith, C. Pasquini, S. Loos, P. Chernev, K. Klingan, P. Kubella, M. R. Mohammadi, D. González-Flores, H. Dau, *Energy Environ. Sci.* **2018**, *11*, 2476-2485; o) B. M. Hunter, N. B. Thompson, A. M. Müller, G. R. Rossman, M. G. Hill, J. R. Winkler, H. B. Gray, *Joule* **2018**, *2*, 747-763.

[5] a) L. Francàs, S. Corby, S. Selim, D. Lee, C. A. Mesa, R. Godin, E. Pastor, I. E. L. Stephens, K.-S. Choi, J. R. Durrant, *Nat. Commun.* **2019**, *10*, 5208; b) M. Steimecke, G. Seiffarth, M. Bron, *Anal. Chem.* **2017**, *89*, 10679-10686; c) M. W. Louie, A. T. Bell, *J. Am. Chem. Soc.* **2013**, *135*, 12329-12337.

[6] J. Yu, B. R. Martin, A. Clearfield, Z. Luo, L. Sun, *Nanoscale* **2015**, *7*, 9448-9451.

[7] F. Song, X. Hu, *Nat. Commun.* **2014**, *5*, 4477..

[8] a) H. Bode, K. Dehmelt, J. Witte, *Electrochim. Acta* **1966**, *11*, 1079-IN1071; b) D. A. Corrigan, *J. Electroche. Soc.* **1987**, *134*, 377-384.

[9] L. Trotochaud, S. L. Young, J. K. Ranney, S. W. Boettcher, *J. Am. Chem. Soc.* **2014**, *136*, 6744-6753.

[10] a) M. Merrill, M. Worsley, A. Wittstock, J. Biener, M. Stadermann, *J. Electroanal. Chem.* **2014**, *717*, 177-188; b) E. Flores, P. Novák, E. J. Berg, *Front. Energy Res.* **2018**, *6*, 82; c) D. Chen, X. Xiong, B. Zhao, M. A. Mahmoud, M. A. El‐Sayed, M. Liu, *Adv. Sci.* **2016**, *3*, 1500433.

[11] O. Diaz-Morales, D. Ferrus-Suspedra, M. T. M. Koper, *Chem. Sci.* **2016**, *7*, 2639-2645.

[12] a) W. Ye, X. Fang, X. Chen, D. Yan, *Nanoscale* **2018**, *10*, 19484-19491; b) O. Diaz-Morales, I. Ledezma-Yanez, M. T. Koper, F. Calle-Vallejo, *ACS Catal.* **2015**, *5*, 5380-5387.

[13] a) J. D. Michael, E. L. Demeter, S. M. Illes, Q. Fan, J. R. Boes, J. R. Kitchin, *J. Phys. Chem. C* **2015**, *119*, 11475-11481; b) A. C. Garcia, T. Touzalin, C. Nieuwland, N. Perini, M. T. Koper, *Angew. Chem. Int. Ed.* **2019**, *58*, 12999-13003; *Angew. Chem.* **2019**, *131*, 13133-13137.

[14] Q. Kang, L. Vernisse, R. C. Remsing, A. C. Thenuwara, S. L. Shumlas, I. G. McKendry, M. L. Klein, E. Borguet, M. J. Zdilla, D. R. Strongin, *J. Am. Chem. Soc.* **2017**, *139*, 1863-1870.

[15] J. Zaffran, M. Nagli, M. Shehadeh, M. C. Toroker, *Theor. Chem. Acc.* **2018**, *137*, 3.

[16] M. M. Waegele, C. M. Gunathunge, J. Li, X. Li, *J. Chem. Phys.* **2019**, *151*, 160902.

[17] W. Jin, H. Du, S. Zheng, H. Xu, Y. Zhang, *J. Phys. Chem. B* **2010**, *114*, 6542-6548.

[18] a) F. Song, M. M. Busch, B. Lassalle-Kaiser, C.-S. Hsu, E. Petkucheva, M. I. Bensimon, H. M. Chen, C. Corminboeuf, X. Hu, *ACS cent. Sci.* **2019**, *5*, 558-568; b) S. Anantharaj, S. Kundu, *ACS Energy Lett.* **2019**, *4*, 1260-1264.

[19] D. Zhou, S. Wang, Y. Jia, X. Xiong, H. Yang, S. Liu, J. Tang, J. Zhang, D. Liu, L. Zheng, Y. Kuang, X. Sun, B. Liu, *Angew. Chem. Int. Ed.* **2019**, *58*, 736-740; *Angew. Chem.* **2019**, *131*, 746-750.

[20] a) A. D. Doyle, M. Bajdich, A. Vojvodic, *Catal. Lett.* **2017**, *147*, 1533-1539; b) J. Zaffran, M. B. Stevens, C. D. Trang, M. Nagli, M. Shehadeh, S. W. Boettcher, M. Caspary Toroker, *Chem. Mater.* **2017**, *29*, 4761-4767.

[21] A. Indra, P. W. Menezes, N. R. Sahraie, A. Bergmann, C. Das, M. Tallarida, D. Schmeißer, P. Strasser, M. Driess, *J. Am. Chem. Soc.* **2014**, *136*, 17530-17536.

Entry for the Table of Contents

Insert graphic for Table of Contents here. ((Please ensure your graphic is in **one** of following formats))

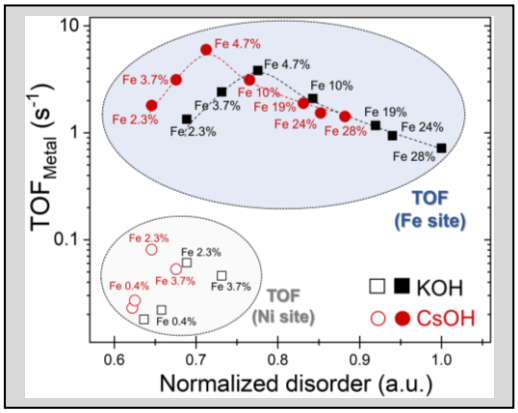

Insert text for Table of Contents here. ((The Table of Contents text should give readers a short preview of the main theme of the research and results included in the paper to attract their attention into reading the paper in full. The Table of Contents text **should be different from the abstract** and should be no more than 450 characters including spaces.)) Turnover frequencies (TOFs) of both Ni and Fe sites in OER catalyzed by a series of Ni and NiFe layered double hydroxides (LDHs) have been determined. Effects of structural disorder of NiOOH lattice have been revealed.

Institute and/or researcher Twitter usernames: ((optional))